Vibrationally resolved photoelectron spectroscopy of the first row transition metal and C_3 clusters: MC_3^- (M=Sc, V, Cr, Mn, Fe, Co, and Ni)

Lai-Sheng Wang[a] and Xi Li
Department of Physics, Washington State University, 2710 University Drive, Richland, Washington 99352 and W. R. Wiley Environmental Molecular Sciences Laboratory, Pacific Northwest National Laboratory, MS K8-88, Richland, Washington 99352

(Received 13 August 1999; accepted 30 November 1999)

We report photoelectron spectra of the MC_3^- clusters for M=Sc, V, Cr, Mn, Fe, Co, and Ni at two photon energies, 355 and 266 nm. Vibrational structure is resolved for the ground and excited state detachment transitions for all the clusters except for CoC_3^- and NiC_3^-. Electron affinity (EA) and vibrational frequencies for the MC_3 clusters are obtained. Complicated low-lying excited state features are observed for all the species. We find that the trend of the EA across the $3d$ series for the MC_3 clusters is similar to that of the MC_2 species. The vibrational frequency is found to increase from ScC_3 to TiC_3 and then decreases monotonically to the right of the $3d$ series. Preliminary density functional theory calculations are performed on all the MC_3 and MC_3^- clusters at several initial geometries and spin multiplicities. We find that the ground states of all the MC_3 and MC_3^- species have C_{2v} ring structures. The calculated M–C stretching frequency for all the MC_3 species is in good agreement with the experimental measurement, lending credence to the obtained C_{2v} structure. © *2000 American Institute of Physics.* [S0021-9606(00)00308-1]

I. INTRODUCTION

The interaction of carbon with transition metals is important in understanding a range of novel nanomaterials from endohedral fullerenes for the rare earth elements,[1] to met-cars for the early transition metals,[2] to the catalytic growth of carbon nanotubes by the late transition metals.[3] Our goal has been to understand the chemical bonding and structure of the small transition metal–carbon clusters to help elucidate the formation mechanisms of these different nanomaterials. Our major experimental technique has been size-selected anion photoelectron spectroscopy (PES), which can yield electronic and vibrational information for the small transition metal–carbon clusters. One of our research strategies is to study systematically small metal–carbon clusters across the $3d$ series. The systematic information is useful, not only to uncover periodic trend, but also to provide experimental spectroscopic data, which will be valuable to theoretical investigations.

For the metal–carbon clusters, we have focused considerable effort on obtaining electronic structure information of met-cars and their growth mechanisms.[4–7] We have also studied a series of small titanium–carbon clusters, TiC_x^- ($x=2-5$).[8] In a recent report,[9] we presented a systematic investigation of the transition metal–C_2 clusters, MC_2. We found that both the periodic trend of the electron affinity (EA) and M–C vibrational frequency of the MC_2 clusters are similar to that of the corresponding diatomic metal oxides. We suggested that the M–C_2 bonding is rather ionic and that the MC_2 clusters can be viewed approximately as $M^{2+}C_2^{2-}$. In the current work, we report our systematic investigation of the MC_3^- clusters from M=Sc to Ni. We are interested in the question of whether the same periodic trends exist in the MC_3 clusters and how the cluster structures and bonding evolve from MC_2 to MC_3.

Among the MC_3 clusters presented here, only FeC_3 has been studied previously.[10,11] We reported a PES spectrum of FeC_3^- at somewhat lower resolution and also did density functional theory (DFT) calculations.[10] Our calculations within the local density approximation (LDA) gave a linear structure for both the anion and neutral. A more recent calculation by Nash, Rao, and Jena gave a C_{2v} ring structure for FeC_3 neutral.[11] Other experimental studies of MC_3 clusters include PES studies of TiC_3^- by us[8] and LaC_3^- by Suzuki *et al.*[12] We proposed a C_{2v} ring structure for TiC_3 based on the similar EAs of all the TiC_x series of clusters that we studied. The C_{2v} structure of TiC_3 has been confirmed by recent DFT calculations by Sumathi and Hendrickx.[13] Other MC_3 clusters studied theoretically involve YC_3 and LaC_3, both of which have been concluded to have C_{2v} ring structures.[14–18]

In the present paper, we report vibrationally resolved PES spectra of MC_3^- for M=Sc, V, Cr, Mn, Fe, Co, and Ni at 355 and 266 nm. We indeed find that the trends of EA and M–C vibrational frequency across the $3d$ series for the MC_3 clusters are similar to those of the MC_2 series that we reported previously. To understand the structural and bonding properties of the MC_3 clusters, we further carried out preliminary DFT calculations for both the anions and neutrals. We find that all of the MC_3 clusters appear to have the C_{2v} ring structure. Our calculated M–C stretching frequency for the C_{2v} MC_3 clusters is in good agreement with the experimental measurements.

[a]Author to whom all correspondence should be addressed; electronic mail: ls.wang@pnl.gov

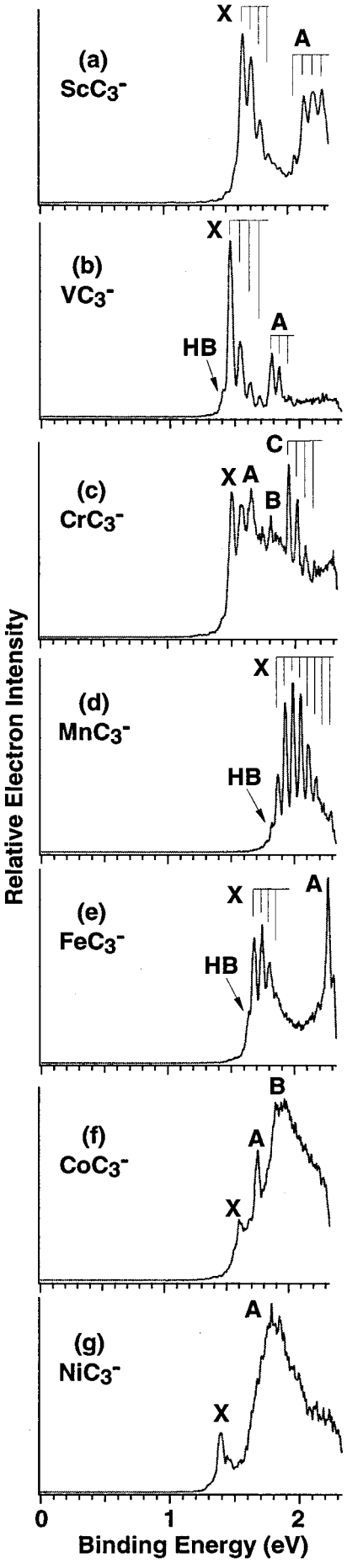

FIG. 1. Photoelectron spectra of MC_3^- at 532 nm.

II. EXPERIMENT

The experiments were performed using a magnetic-bottle PES apparatus with a laser vaporization cluster source. Details of the experiments have been published elsewhere;[19,20] only a brief description is given here. The MC_3^- anions were produced by laser vaporization of the respective metal targets with a helium carrier gas containing 5% CH_4. Metal–carbon mixed clusters were synthesized through plasma reactions between laser-ablated metal atoms and CH_4. Cluster species, entrained in the helium carrier gas, underwent a supersonic expansion and formed a collimated beam with a 6-mm-diam skimmer. The anions were extracted perpendicularly from the cluster beam into a time-of-flight (TOF) mass spectrometer. The anions of interest were mass selected and decelerated before crossing with a detachment laser beam. Two photon energies (532 nm–2.331 eV; 355 nm–3.496 eV) from a *Q*-switched Nd:YAG laser were used for the current experiments. The photoemitted electrons were collected by the magnetic bottle at nearly 100% efficiency and analyzed in a 3.5-m-long TOF tube. Photoelectron TOF spectra were collected at a 10 Hz repetition rate and converted to electron binding energies (BEs) calibrated by the known spectrum of Rh^-. VC_3^- and CrC_3^- were also produced using the respective solid carbide targets with a pure helium carrier gas. The same PES spectra were obtained as using pure metal targets and a CH_4-containing He carrier gas. The resolution of the magnetic-bottle electron analyzer

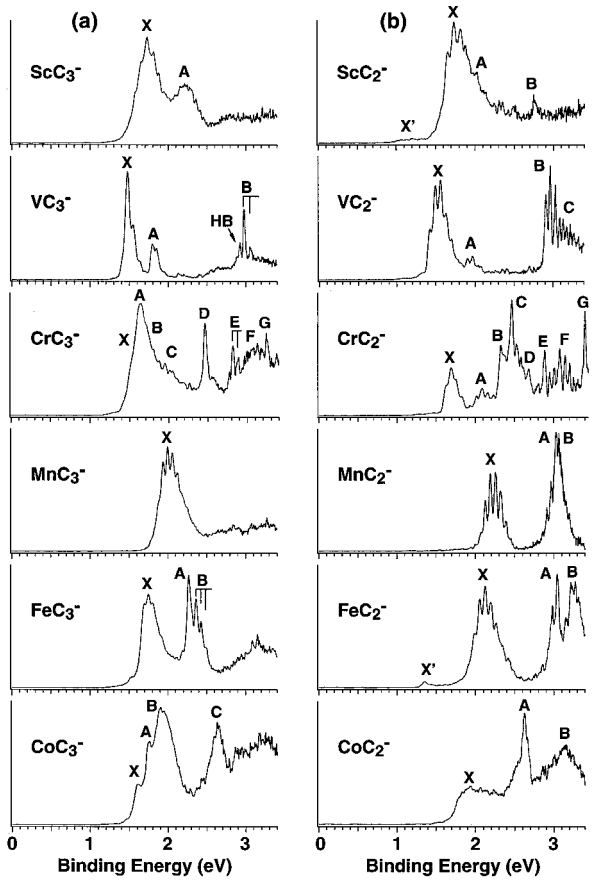

FIG. 2. Photoelectron spectra of MC_3^- at 355 nm, in comparison to those of the MC_2^- species from Ref. 9.

TABLE I. Observed adiabatic (ADE) and vertical (VDE) binding energies, vibrational frequencies, and low-lying electronic states for ScC_3, VC_3, CrC_3, MnC_3, FeC_3, CoC_3, and NiC_3.

		ADE (eV)[a]	VDE (eV)	ΔE (eV)[b,c]	Vib. freq. (cm^{-1})[c]
ScC_3	*X*	1.64 (0.02)		0	560 (30)
	A	2.06 (0.02)	2.28(0.02)	0.42(0.02)	600 (50)
VC_3	*X*	1.47 (0.02)		0	600 (30)
	A	1.79 (0.02)		0.32(0.02)	450 (50)
	B	2.98 (0.03)		1.51(0.03)	600 (50)
CrC_3	*X*	1.50 (0.02)		0	560 (60)
	A	1.65 (0.03)		0.15(0.02)	
	B	1.81 (0.03)		0.31(0.02)	
	C	1.95 (0.03)		0.45(0.02)	540 (30)
	D	2.46 (0.03)		0.96(0.02)	
	E	2.82 (0.04)		1.32(0.03)	500 (50)
	F	~3			
	G	3.24 (0.04)		1.74(0.03)	
MnC_3	*X*	1.87 (0.02)	1.99(0.02)	0	490 (20)
FeC_3	*X*	1.68 (0.02)	1.74(0.02)	0	480 (40)
	A	2.27 (0.02)		0.59(0.02)	[350 (50)]
	B	2.36 (0.02)		0.68(0.02)	500 (30)
CoC_3	*X*	1.55 (0.06)	1.60(0.06)	0	
	A		1.75(0.05)	(0.15)	
	B		1.9(0.1)	(0.3)	
	C		2.63(0.06)	(1.03)	
NiC_3	*X*	1.39 (0.05)		0	480 (60)
	A		1.8(0.1)	(0.4)	

[a]The ADE of the ground state feature (*X*) represents the adiabatic electron affinity.
[b]The excitation energies relative to the ground state (*X*).
[c]Relative energies were measured more accurately.

was about $\Delta E/E \sim 2\%$, i.e., ~20 meV for 1 eV electrons. The further improvement of our magnetic-bottle apparatus can be found in a recent publication.[21]

III. RESULTS AND DISCUSSION

The PES spectra at 532 nm are shown in Fig. 1 for all seven MC_3^- species (M=Sc, V, Cr, Mn, Fe, Co, and Ni). The 355 nm spectra are shown in Fig. 2, where the spectra of the corresponding MC_2^- species are also shown for comparison. The observed detachment transitions are labeled with letters and the vertical lines represent resolved vibrational structures. The observed binding energies and vibrational frequencies are summarized in Table I for all the seven MC_3 species investigated currently.

A. ScC_3^-

The 532 nm spectrum exhibits two vibrationally resolved bands [Fig. 1(a)]. The ground state vibrational progression (*X*) shows a spacing of 560 (30) cm^{-1}. The 0–0 transition of the *X* band at 1.64 eV defines the adiabatic EA of ScC_3. The *A* band, with a vibrational spacing of 600 (50) cm^{-1}, was cut off due to the low photon energy. At 355 nm [Fig. 2(a)], considerable hot band intensity was observed at the low BE side. The 355 nm spectrum was broad, with weak signals through the entire high BE side, probably due to closely spaced low-lying electronic states of ScC_3.

It is interesting to note that our measured EA of 1.64 (2) eV for ScC_3 is practically identical to our previously measured EA of 1.65 (3) eV for ScC_2. The PES spectra of the two species are also somewhat similar (Fig. 2), except that the *X*–*A* separation in ScC_2 is smaller (0.29 eV) compared to the *X*–*A* separation of 0.42 eV in ScC_3 (Table I). In addition, the ground state vibrational progression in the spectra of ScC_3^- is shorter compared to that in ScC_2^-, suggesting that the geometry changes between the anion and neutral in the C_3 cluster is less than that in the C_2 cluster. We also note that the vibrational frequency observed in ScC_3 (560 cm^{-1}, Table I) is smaller than that in ScC_2 (670 cm^{-1}).

B. VC_3^-

Two well-resolved vibrational progressions were observed in the 532 nm spectra of VC_3^- [Fig. 1(b)]. The *X* band gives a vibrational spacing of 600 cm^{-1}, whereas the *A* band yields a smaller spacing of 450 cm^{-1}, as shown in Table I. A hot band (HB) feature is also visible in the spectrum. The 0–0 transition yields an adiabatic EA of 1.47 eV for VC_3. The 355 nm spectrum [Fig. 2(a)] showed three extra sharp peaks near 3 eV. We identified these features as a vibrational progression (*B*) with a HB feature, as indicated. The *B* band gives a vibrational spacing of 600 cm^{-1}, identical to that of the ground state. There are also weak features between 2 and 2.8 eV, which we could not identify definitively. The HB features yielded a vibrational frequency of 420 (50) cm^{-1} for the VC_3^- anion.

The EA of VC_3 (1.47 eV) is only slightly higher than that of VC_2 (1.42 eV). As seen in Fig. 2, there is considerable similarity between the spectra of the two clusters, except that the vibrational progressions in the VC_2^- spectrum are all longer than that in the VC_3^- spectrum. The latter subtle difference suggests that there are less geometry changes between the anion and neutral in the C_3 cluster than that in the C_2 cluster, analogous to the corresponding Sc species. How-

ever, in contrast to the Sc species, we observed that the ground state vibrational frequency of VC_3 (600 cm^{-1}) is actually slightly larger than that of VC_2 (550 cm^{-1}).

C. CrC_3^-

The spectra of CrC_3^- seemed to be much more complicated than those of VC_3^-. The 532 nm spectrum [Fig. 1(c) reveals several overlapping features. One vibrational progression (C) can be clearly recognized with a spacing of 540 cm^{-1}. Between the threshold and the C band, we tentatively identified three overlapping states, but could not obtain the vibrational spacings, except for the ground state, for which we estimated a vibrational spacing of ~560 cm^{-1}. The 0–0 transition yields an adiabatic EA of 1.50 eV for CrC_3. In the 355 nm spectrum [Fig. 2(a)], the relative intensities of those features observed in the 532 nm spectrum appeared to be changed significantly. In particular, the intensities of the X and C band were apparently reduced, whereas that of the A band was enhanced. Several more features were observed in the 355 nm spectrum at higher BE. A sharp feature (D) was observed at 2.46 eV. A short vibrational progression (E) with a spacing of ~500 cm^{-1} could be recognized at ~2.8 eV. More overlapping features exist at even higher BEs (F and G) in the 355 nm spectrum.

Our measured EA for CrC_3 (1.50 eV) is actually slightly smaller than that for CrC_2 (1.63 eV). There were also obvious similarities between the spectra of the two species (Fig. 2). In particular, both species seemed to produce the most complicated spectra in each series with many low-lying excited states observed for the corresponding neutrals.

D. MnC_3^-

The 532 nm spectrum of MnC_3- [Fig. 1(d)] revealed one broad vibrational progression with a spacing of 490 cm^{-1}. The 0–0 transition yielded an adiabatic EA of 1.87 eV for MnC_3. The 355 nm spectra [Fig. 2(a)] gave almost continuous signals at the high BE side. But we could not identify any feature definitively, probably suggesting a high density of low-lying states. A HB feature was clearly observed in the 532 nm spectrum, yielding a vibrational frequency of 370 (40) cm^{-1} for the MnC_3^- anion.

The broad vibrational progression in the MnC_3^- spectrum is very similar to that in the MnC_2^- spectrum, as shown in Fig. 2. The EA of MnC_3 (1.87 eV) is smaller than that of MnC_2 (2.12 eV) whereas they both have similar ground state vibrational frequencies, 490 cm^{-1} for MnC_3 and 520 cm^{-1} for MnC_2. The broad vibrational progression in the MnC_x^- spectra indicated that there are large geometry and bonding changes between the anion and neutral ground states in these species. The large difference between the vibrational frequencies of MnC_3^- and MnC_3 is consistent with these changes.

E. FeC_3^-

The 532 nm spectrum FeC_3^- [Fig. 1(e)] revealed one well-resolved ground state vibrational progression (X) with a spacing of 480 cm^{-1} and a sharp feature (A) at 2.27 eV. The 0–0 transition of the ground state progression yielded an adiabatic EA of 1.68 eV for FeC_3. There seemed to be another component just beyond the sharp A peak, which could be the second component of a short vibrational progression, giving a vibrational spacing of ~350 cm^{-1} for the A band. At 355 nm [Fig. 2(a)], more features were observed at the high BE side. Several sharp peaks (B) were revealed just beyond the 532 nm photon energy. However, these new features did not belong to the vibrational progression starting from the A peak; rather they were identified as a new progression with a spacing of 500 cm^{-1}. More features exist beyond 2.7 eV, but could not be clearly resolved. A HB feature was observed in the 532 nm spectrum, giving a vibrational frequency of 330 (40) cm^{-1} for the FeC_3^- anion.

We previously obtained the 355 nm spectrum of FeC_3^- at a lower instrumental resolution,[10] where no vibrational structures were resolved for the ground state. The current vibrationally resolved spectrum at 532 nm not only yielded the ground state vibrational frequency, but also allowed the EA of FeC_3 to be more accurately measured. Due to the lower resolution, the A and B features were identified mistakenly as a singly vibrational progression previously. The current data clearly showed that the A feature does not belong to the B progression. The A–B separation was 90 meV (Table I), which is much larger than the average spacing of the B progression (500 cm^{-1} or 62 meV). The A state probably represents removal of a nonbonding electron, thus giving a very short vibrational progression. The tentatively measured vibrational frequency of the A state (~350 cm^{-1}) is similar to that of the anion (~330 cm^{-1}), providing indirect evidence supporting the identification and assignment of the A state.

F. CoC_3^-

The spectra of CoC_3^- are much more congested with no vibrational structures resolved. The 532 nm spectrum [Fig. 1(f)] revealed two sharp features (X and A), followed by a broad band (B). The adiabatic EA was estimated from the X feature as 1.55 eV. The 355 nm spectrum [Fig. 2(a)] showed more broad features at higher BE. A broad feature C could be recognized around 2.6 eV.

The onset of broad features and lack of resolved vibrational features in the spectra of CoC_3^- are similar to that in CoC_2^-. The spectra of CoC_3^- and CoC_2^- also exhibit certain similarity, as can be seen in Fig. 2.

G. NiC_3^-

The 532 nm spectrum of NiC_3^- [Fig. 1(g)] revealed a weak feature (X) and a broad feature (A). The weak X band seemed to show a short vibrational progression with a spacing of ~480 cm^{-1}. The 0–0 transition of the X band yielded an adiabatic EA of 1.39 eV for NiC_3. The 355 nm spectrum of NiC_3^-, which is not shown, revealed only an additional broad and continuous feature starting at ~2.6 eV, suggesting probably a very high density of low-lying states for the NiC_3 cluster, similar to that in CoC_3. In our previous investigation of the MC_2^- species,[9] NiC_2^- was omitted because of difficulty in producing it in our laser vaporization source.

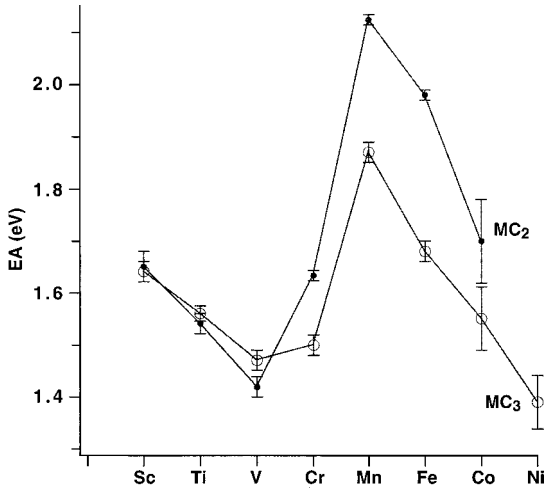

FIG. 3. Electron affinities (EA) of the first row transition metal–C_3 clusters, compared to those of the dicarbides (MC_2).

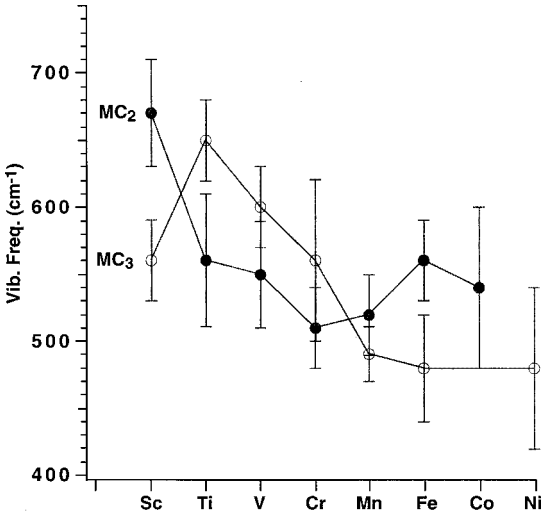

FIG. 4. Ground state vibrational frequencies of the first row transition metal–C_3 clusters, compared to those of the dicarbides (MC_2).

H. Periodic trends of EAs and ground state vibrational frequencies

The adiabatic EAs of the MC_3 clusters are plotted in Fig. 3 and compared to that of the corresponding MC_2 clusters. The EAs for the TiC_x and the MC_2 species are from our previous publications.[8,9] We found that the periodic trend of the EAs for the MC_3 clusters across the $3d$ series is identical to that of the MC_2 species, with a minimum at VC_3 and a maximum at MnC_3. We note that the EAs of the MC_2 and MC_3 clusters are all smaller than that of the corresponding pure carbon clusters, C_2 (3.269 eV)[22] and C_3 (1.995 eV),[23] respectively, while they are all higher than the EAs of the pure metals.[24] Thus we can infer that the extra electron in the MC_x^- clusters is probably shared by the metal and carbon fragments. The observed ground state vibrational progressions in the MC_2 clusters all indicate that the extra electron occupies an antibonding M–C orbital because the observed vibrational frequency for the neutral MC_2 are all higher than that of the anions, as estimated from the hot band features. We further suggested that the M–C_2 bonding is quite ionic, based on the similar trends in EA and vibrational frequency between the MC_2 and corresponding monoxide species. The large EA of C_2 certainly makes it reasonable to have some degree of charge transfer from the metal to C_2 in MC_2. We also observed a ground state vibrational progression for all the MC_3^- clusters except for CoC_3^- and NiC_3^-, suggesting significant geometry changes between the anions and neutrals in the MC_3 species. Based on the hot band features observed, the vibrational frequencies estimated for the anions are also smaller than that of the neutral MC_3. Thus we infer that the extra electron in MC_3^- is also likely to be occupying an antibonding M–C orbital, similar to that in MC_2^-. The similar PES spectra between the MC_3^- and MC_2^- species as shown in Fig. 2 also suggest that there should be some similarities between their structure and bonding. There is probably also some degree of charge transfer from the metal to C_3 in MC_3, but probably less than that in MC_2, considering the smaller EA of C_3 than that of C_2.

Figure 4 shows the trend of the measured vibrational frequencies for the ground state of the MC_3 clusters across the $3d$ series. Based on the previous discussion, the resolved vibration should be due to the M–C symmetric stretching in the MC_3 clusters. Although we could see certain similarity in the overall trend between the MC_3 and MC_2 series, we also found some subtle differences. In particular, we found that the highest M–C frequency in the MC_3 series occurs in TiC_3 whereas in the MC_2 series it occurs in ScC_2. The M–C frequency then decreases steadily from TiC_3 to the right of the $3d$ series. The vibrational frequency trend in the MC_3 series suggests that the TiC_3 cluster has the strongest metal–C bond strength, which then decreases to the right of the $3d$ series. This observation agrees with the general trend of the interaction between carbon and the transition metals across the $3d$ series.

IV. PRELIMINARY THEORETICAL CALCULATIONS

As mentioned in Sec. I, the only $3d$ MC_3 clusters that have been studied theoretically are TiC_3 and FeC_3. We suggested a ring structure for TiC_3 in our previous study of the TiC_x clusters,[8] which has been confirmed by DFT calculations by Sumathi and Hendrickx.[13] The structure of FeC_3 is uncertain: while our previous DFT calculation suggested a linear structure,[10] the recent calculation by Nash, Rao, and Jena suggested a C_{2v} ring structure.[11] In order to obtain systematic structural information, we carried out a preliminary theoretical study on all the MC_3 clusters investigated here except CoC_3 and NiC_3. The current calculations indeed suggest a C_{2v} ring structure for all the MC_3 species.

The calculations presented here were performed using the GAUSSIAN 94 package.[25] Energy calculations and geometry optimizations were carried out using the B3LYP density functional method,[26] in which the Becke's three-parameter exchange functional[27] and the Lee–Yang–Parr correlation functional[28] were used. Vibrational frequencies of the neutral clusters were calculated at the DFT level in order to characterize the nature of the stationary points and com-

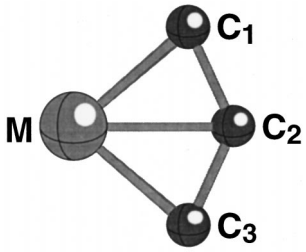

FIG. 5. Schematic structure of the MC_3 clusters. See detailed structural parameters from the theoretical calculations for the different clusters in Table II.

pare with the experimental results. The basis sets used are 6-311+G($3df$) for the metals and carbon, as denoted in the GAUSSIAN 94 package.

For each species, we calculated both the anion and neutral with several spin multiplicities and three initial structures: (1) a C_{2v} ring structure; (2) a linear MCCC structure; and (3) a C_{2v} structure in which the metal is bonded to two carbons of a triangular C_3. In all cases, we found that the C_{2v} ring structure is a true minimum through frequency calculations and has the lowest energy among the three structures. Figure 5 shows a schematic structure for this C_{2v} species and Table II lists the spin multiplicities and the structural parameters for these clusters. For both ScC_3^- and VC_3^-, we found a nearly degenerate state with different spin multiplicities. The calculated M–C symmetric stretching frequency for each species is also listed in Table II and compared to the experimental measurements. The parameters for TiC_3 are also listed in Table II for comparison. The theoretical adiabatic electron affinity for each species, obtained from the total energy difference between the anion and neutral, is also listed in Table II.

Several observations can be made from the data presented in Table II. First, the calculated vibrational frequency in all cases seems to agree well with the experimental measurements. Second, the M–Cl bond length is longer in the anions than in the neutrals, consistent with our observations that a vibrational progression in the ground state was observed in all PES spectra and that the extra electron in the anions occupies an antibonding M–C orbital. Third, the magnitudes of changes in the M–Cl bond length between the anions and neutrals are consistent with the Franck–Condon envelope observed in each case. For example, the largest change occurs in the MnC_3/MnC_3^- pair, consistent with the fact that the MnC_3^- spectra exhibited the broadest Franck–Condon envelope. Fourth, the theoretical electron affinity is also in reasonable agreement with the experimental measurement (Table I), considering the theoretical method used. Although it is known that the DFT method used gives poor energetics, the trend of the calculated EA is consistent with the experimental observation.

While we cannot claim if the DFT method used here is adequate for these complicated systems, the agreements between the experiment and theory do lend some credence to the C_{2v} ring structure for the MC_3 clusters. The C_{2v} structure and the spin multiplicity for FeC_3 in fact agree with those obtained previously by Nash, Rao, and Jena.[11] The C_{2v} ring structure for ScC_3 is also reasonable since the isoelectronic YC_3 and LaC_3 clusters are known to have the same structure from previous theoretical studies.[14–18]

The trend of the EA shown in Fig. 3 is interesting. It is instructive to speculate on its origin since the EA is related to the electronic structure and bonding of the MC_3 clusters. From the previous discussion, we know that the extra electron in the MC_3^- anions all occupies a slightly antibonding orbital, which should be primarily of $3d$ character. One

TABLE II. Calculated structural parameters for the ground state C_{2v} MC_3 and MC_3^- clusters (see Fig. 5), spin multiplicity (S), and M–C stretching vibrational frequency and electron affinities. The full set of calculated vibrational frequencies in cm^{-1} for each cluster are as follows: ScC_3: a_1=**594**, 701, 1729; b_1=649; b_2=404, 1457. VC_3: a_1=**600**, 835, 1307; b_1=576; b_2=440, 1542. CrC_3: a_1=**556**, 810, 1314; b_1=501; b_2=440, 1487. MnC_3: a_1=**498**, 723, 1285; b_1=471; b_2=395, 1467. FeC_3: a_1=**469**, 727, 1306; b_1=448; b_2=437, 1496.

					ν_{M-C} (cm^{-1})		
	S	M–C_1 (Å)	M–C_2 (Å)	C_1–C_2(Å)	Theo.	Expt.	EA (eV)[e]
ScC_3	2	2.027	2.108	1.322	594	560 (30)	1.99
ScC_3^-	3[a]	2.105	2.128	1.322			
TiC_3	1[b]	1.878[b]	1.962[b]	1.346[b]	686[b]	650(30)[c]	
VC_3	2	1.834	1.930	1.328	600	600 (30)	1.40
VC_3^-	3[d]	1.909	1.993	1.330			
CrC_3	3	1.834	1.938	1.334	556	560 (60)	1.26
CrC_3^-	4	1.905	1.982	1.346			
MnC_3	4	1.887	1.957	1.334	498	490 (20)	1.57
MnC_3^-	5	1.992	2.032	1.339			
FeC_3	3	1.829	1.927	1.334	469	480 (40)	1.44
FeC_3^-	4	1.921	2.002	1.340			

[a]A singlet state is only 0.022 eV higher with the same structural parameters.
[b]From Ref. 13.
[c]From Ref. 8.
[d]A singlet state is only 0.04 eV higher with V–C_1=1.886 Å, V–C_2=1.966 Å, and C_1–C_2=1.331 Å.
[e]Electron affinity is obtained from the total energy difference between the anion and neutral.

would expect a decrease of EA from left to right across the $3d$ series in the MC_3 clusters due to the electron–electron repulsion and the antibonding nature of the d orbitals. However, a maximum is observed at MnC_3, which is probably caused by a large contribution of exchange interactions due to the high spin multiplicity in MnC_3^-.

Finally, we suggest that further and more accurate theoretical calculations on these MC_3 clusters would be desirable to confirm the current observations and preliminary conclusions. In particular, a detailed and systematic investigation including CoC_3 and NiC_3 would be interesting. The broad and unresolved PES spectra for these two species seemed to show abrupt changes, in comparison to the spectra of the earlier MC_3^- species, which all showed at least a vibrationally resolved ground state. We speculate that perhaps that could be due to a significant structural or bonding change in the latter. The trend of the M–C vibrational frequency and M–C bond length as shown in Table II both suggest that the M–C bond weakens along the $3d$ series from left to right. Thus, a structural change at some point might be expected when the bending of the C_3 can no longer be compensated by the additional M–C bonding in the C_{2v} ring structure. The trend of the EA is also interesting: while the Ni atom has the highest EA among the $3d$ metals,[24] NiC_3 has the lowest EA among the MC_3 clusters, suggesting that the extra electron is mostly localized on a Ni-based orbital, rather than a Ni–C-based orbital. In any case, further theoretical studies of the MC_3 clusters would be very desirable to completely elucidate the structural and chemical bonding evolution across the $3d$ series. Such information would be valuable in providing ultimately a molecular level understanding of the different nanomaterials formed between carbon and the $3d$ transition metals across the $3d$ series.

V. CONCLUSIONS

We presented vibrationally resolved photoelectron spectra of MC_3^- for M=Sc, V, Cr, Mn, Fe, Co, and Ni. Electron affinities, low-lying electronic states, and vibrational frequencies for the neutral MC_3 clusters are obtained. The trend of the electron affinities and the electronic structure for the MC_3 species are found to be similar to the MC_2 species. The ground state vibrational frequencies of the MC_3 clusters decreases from TiC_3 to the right of the $3d$ series. Preliminary density functional theory calculations were performed for both the anions and neutrals of the transition metal C_3 clusters, except the Co and Ni clusters, and suggested a C_{2v} ring structure for all the MC_3 species. The calculated M–C frequencies are in good agreement with the experimental measurements. The geometry changes between the C_{2v} anions and neutrals are also consistent with the observation of the ground state vibrational progressions in the cluster photoelectron spectra.

ACKNOWLEDGMENTS

Support of this research by the National Science Foundation (DMR-9622733) is gratefully acknowledged. This work was performed at the W. R. Wiley Environmental Molecular Sciences Laboratory, a national scientific user facility sponsored by DOE's Office of Biological and Environmental Research and located at Pacific Northwest National Laboratory, operated for DOE by Battelle. Assistance in the theoretical calculations by W. Chen is acknowledged. L. S. W. is an Alfred P. Sloan Foundation Research Fellow.

[1] Y. Chai *et al.*, J. Phys. Chem. **95**, 7564 (1991).
[2] B. C. Guo, K. P. Kerns, and A. W. Castleman, Science **255**, 1411 (1992).
[3] S. Iijima and T. Ichihashi, Nature (London) **363**, 603 (1993).
[4] L. S. Wang, S. Li, and H. Wu, J. Phys. Chem. **100**, 19211 (1996).
[5] L. S. Wang and H. Cheng, Phys. Rev. Lett. **78**, 2983 (1997).
[6] S. Li, H. Wu, and L. S. Wang, J. Am. Chem. Soc. **119**, 7417 (1997).
[7] L. S. Wang, X. B. Wang, H. Wu, and H. C. Cheng, J. Am. Chem. Soc. **120**, 6556 (1998).
[8] X. B. Wang, C. F. Ding, and L. S. Wang, Acc. Chem. Res. **101**, 7699 (1997).
[9] X. Li and L. S. Wang, J. Chem. Phys. **111**, 8389 (1999).
[10] J. Fan, L. Lou, and L. S. Wang, J. Chem. Phys. **102**, 2701 (1995).
[11] B. K. Nash, B. K. Rao, and P. Jena, J. Chem. Phys. **105**, 11020 (1996).
[12] S. Suzuki, M. Kohno, H. Shiromaru, Y. Achiba, H. Kietzmann, B. Kessler, G. Gantefor, and W. Eberhardt, Z. Phys. D **40**, 407 (1997).
[13] R. Sumathi and M. Hendrickx, J. Phys. Chem. A **102**, 4883 (1998).
[14] S. Roszak and K. Balasubramanian, J. Phys. Chem. **100**, 8254 (1996).
[15] D. L. Strout and M. B. Hall, J. Phys. Chem. **100**, 18007 (1996).
[16] S. Roszak and K. Balasubramanian, J. Chem. Phys. **106**, 158 (1997).
[17] A. Ayuela, G. Seifert, and R. Schmidt, Z. Phys. D: At., Mol. Clusters **41**, 69 (1997).
[18] Z. J. Wu, Q. B. Meng, and S. Y. Zhang, Chem. Phys. Lett. **281**, 233 (1997).
[19] L. S. Wang, H. S. Cheng, and J. Fan, J. Chem. Phys. **102**, 9480 (1995).
[20] L. S. Wang and H. Wu, in *Advances in Metal and Semiconductor Clusters. IV. Cluster Materials*, edited by M. A. Duncan (JAI, Greenwich, 1998), p. 299.
[21] L. S. Wang, C. F. Ding, X. B. Wang, and S. E. Barlow, Rev. Sci. Instrum. **70**, 1957 (1999).
[22] K. M. Ervin and W. C. Lineberger, J. Am. Chem. Soc. **95**, 1167 (1991).
[23] D. W. Arnold, S. E. Bradforth, T. N. Kitsopoulos, and D. M. Neumark, J. Chem. Phys. **95**, 8753 (1991).
[24] M. J. Nadeau, M. A. Garwan, X. L. Zhao, and A. E. Litherland, Nucl. Instrum. Methods Phys. Res. B **123**, 521 (1997).
[25] GAUSSIAN 94 (revision A.1). M. J. Frisch, G. M. Trucks, H. B. Schlegel, P. M. W. Gill, B. G. Johnson, M. A. Robb, J. R. Cheeseman, T. A. Keith, G. A. Petersson, J. A. Montgomery, K. Raghavachari, M. A. Al-Laham, V. G. Zakrzewski, J. V. Ortiz, J. B. Foresman, J. Cioslowski, B. B. Stefanov, A. Nanayakkara, M. Challacombe, C. Y. Peng, P. Y. Ayala, W. Chen, M. W. Wong, J. L. Andres, E. S. Replogle, R. Gomperts, R. L. Martin, D. J. Fox, J. S. Binkley, D. J. Defrees, J. Baker, J. J. P. Stewart, M. Head-Gordon, C. Gonzales, and J. A. Pople, Gaussian, Inc., Pittsburgh, PA, 1995.
[26] R. P. Parr and W. Yang, *Density Functional Theory of Atoms and Molecules* (Oxford University Press, Oxford, 1989).
[27] A. D. Becke, J. Chem. Phys. **98**, 5648 (1993).
[28] C. Lee, W. Yang, and R. G. Parr, Phys. Rev. B **37**, 785 (1988).